JOTCS A
Journal of the Turkish Chemical Society
Section: A
Chemistry

TURKISH CHEMICAL SOCIETY

# Adsorption of Ethylene and 1-methylcyclopropene (1-MCP) on Al-doped Graphene Structure: A DFT Study for Gas Sensing Application

**Fatma Aydin[1*], Kivanc Sel[2*]**

[1]Department of Chemistry, Faculty of Sciences, Çanakkale Onsekiz Mart University, 17100 Çanakkale, Turkey.
[2]Department of Physics, Faculty of Sciences, Çanakkale Onsekiz Mart University, 17100 Çanakkale, Turkey.

**Abstract:** Ethylene is the ripening hormone of fruits and vegetables. 1-Methylcyclopropene (1-MCP) is used as the inhibitor of the ethylene actions for extending the postharvest shelf life of the plants. To control the ripening and extending the shelf life of the plants, the adsorption characteristics of ethylene and 1-MCP on Al-doped graphene structure (AlG) were investigated as a gas sensing application by density functional theory (DFT) calculations. The geometric structures were optimized, HOMO and LUMO, energy gap, adsorption energies, the density of states (DOS), electrostatic potential (ESP) and the global reactivities were calculated for different distances between the adsorbed ethylene or 1-MCP and the adsorbent AlG. Chemisorption and physisorption interactions were analyzed. For the chemisorption process of ethylene and 1-MCP on AlG, the adsorption energies were 19.34 kJ/mol and 56.53 kJ/mol, respectively. Whereas for the physisorption process, the adsorption energies of ethylene and 1-MCP were -60.16 kJ/mol and -7.32 kJ/mol, respectively. As a result, it was presented that the AlG structure has sufficient characteristics to be a good adsorbent and a gas sensor of ethylene and 1-MCP.

**Keywords:** Ethylene, 1-methylcyclopropene (1-MCP), Al-doped graphene, Density functional theory, Gas sensor.

**Submitted:** May 31, 2024. **Accepted:** September 25, 2024.

**Cite this:** Aydin F, Kivanc S. Adsorption of Ethylene and 1-methylcyclopropene (1-MCP) on Al-doped Graphene Structure: A DFT Study for Gas Sensing Application. JOTCSA. 2024;11(4): 1535-44.

**DOI:** https://doi.org/10.18596/jotcsa.1492945

***Corresponding author's E-mail:** faydin@comu.edu.tr, kivanc@comu.edu.tr

## 1. INTRODUCTION

Ethylene is widely known as the phytohormone responsible for the ripening of fruits and vegetables and its involvement in plant growth and development processes. It is naturally produced in plants via biochemical reactions defined as the Yang cycle (1). Additionally, ethylene gas added to the environment is also used in ripening rooms under modified atmosphere conditions. On the other hand, to prevent unwanted ripening the ethylene level better be continuously monitored inside the conservation chambers to maintain the appropriate storage conditions and to extend the shelf life of fruits and vegetables (2). Fruit suppliers will need information to reduce economic losses by control ripening time during fruit storage. For this purpose, the use of practical and sensitive sensors to be developed will be more efficient in completing the processes (3).

1-Methylcyclopropene (1-MCP) ($C_4H_6$) has been developed commercially and is used as a synthetic plant regulator. It is a cycloalkene compound and exists as a gas at room temperature (4). Since it inhibits the ethylene receptor, it is used to delay the ripening and softening process of the plants by reducing the respiration rate. Due to the use of 1-MCP for some fruits, color development slows down compared to those that are not used (5,6). It not only significantly reduces the respiration of the plants but also keeps the product hardness, brittleness, color, flavor, aroma and nutrients. As a result of this, the use of 1-MCP in the post-harvest preservation of fruits and vegetables has become widespread. On the other hand, no toxic properties and no detectable odor of its use have been reported (7-10).

There are many studies in the qualitative determination of 1-MCP and various chemical reagents are needed for this (11). Due to the physical and chemical properties of the 1-MCP

molecule, such as vapor pressure of 570 mm Hg at 25 °C and molecular weight of 54 g/mol, GC-MS or LC-MS/MS analysis methods are widely used for the analysis of 1-MCP, but effective and accurate quantitative analysis presents difficulties.

However, since the molecular weight of 1-methylcyclopropene is small, the traditional detection method cannot accurately quantify it due to the possibility of interference with trace volatile compounds in fruits and vegetables, and therefore the research needs of sensitive and accurate analysis techniques cannot be met (12). For this reason, since 1-MCP is a gas molecule, the gas sensor to be developed will facilitate the detection process.

Graphene, which is a flat mesh of regular hexagonal rings, is a two-dimensional monolayer structure containing only carbon atoms. Although graphene contains many carbon atoms in two dimensions, it contains only one layer of carbon in the third dimension, making it one of the thinnest materials with the best surface-to-weight ratio. Since its discovery in 2004 (13,14), many theoretical and experimental researches have been carried out on physical or chemical interactions of graphene and various metal-doped graphene structures with various chemicals. Recently, experimental and theoretical gas sensor studies have been reported for the detection of various gases such as $NO_2$, $N_2O$, $H_2O$, HF, $CO_2$ etc. on graphene (15-17).

The Van der walls interaction between the carbon atoms of graphene and the atoms of the adsorbed gas molecule is relatively weaker than the other bonding types. In this respect, this interaction with the atoms of various adsorbed gas molecules could occur within the limit of a relatively close band of energies and/or bonding coordination. On the other hand, metal-doped graphene can interact with various gas molecules by the Van der walls, covalent and especially coordinate covalent bonding types due to their Lewis acid-base properties. In this respect, metal doping to graphene could improve the sensitivity and selectivity of graphene as a gas sensor. Recent studies have shown that various metal-doped graphene system has much higher adsorption energy and higher net charge transfer value than pure graphene due to Lewis acid-base interaction (18). After graphene is doped with N which has Lewis base propertied, carbon atoms lose electrons while nitrogen atom gain electrons. On the other hand, when graphene is doped with Al, which has Lewis acid properties, carbon gains electrons while aluminum atom loses electrons. The low frequency absorption peak of Al-doped graphene shifts the lower energy compared to pure graphene, making the transitions between π and π* easier. This situation shows that it can lead to an opened gap and reveals the feature of being used as a sensor (19).

Many researches have been focused on metal-doped graphene such as Lewis acid Al, Si, P, B, Ge, Ga, etc. (20-23). Most recently, Al-doped graphene (AlG) was suggested to be a promising structure as a novel molecular sensor to $NH_3$ (24), $NO_2$ and $N_2O$ (25), CO and $CO_2$ (26), some halo-methane (27), $CH_4$ (28), etc. molecules. The B and N doped graphene have also been investigated for the toxic gaseous such as cyanide, formaldehyde and phosgene (29-31). Moreover, the interactions of various molecules such as acrolein (32), guanine (33), cyanuric fluoride (CF) and s-triazine (ST) (34) onto Al-doped graphene have also been examined theoretically.

In this study, due to its importance for post-harvest preservation of some agricultural products, it was considered to design high-performance gas sensor study for the determination of ethylene and 1-MCP molecules. For this purpose, the adsorption of ethylene and 1-MCP molecules on Al-doped graphene structure ($C_2H_4$/AlG and 1-MCP/AlG, respectively) was investigated, using the density functional theory (DFT) calculations. The characterization of ethylene, 1-MCP and AlG and also the adsorption of these molecules on the Al-doped graphene were investigated and compared in detail.

## 2. EXPERIMENTAL SECTION

### 2.1. Computational Details

In this study, the first principles based on DFT calculations were performed (35,36) by using the Quantum ESPRESSO (QE) computational package (QE) (37-39). The ultrasoft pseudopotential (USPP) (40) approach for the core-valence interactions and Perdew-Burke-Ernzerhof (PBE) (41) approximation for the exchange-correlation functional have been applied as implemented in the QE package. A cubic unit cell and the structures were built by using XCRYSDEN (42) and VESTA (43) packages. In order to prevent the interactions between the adjacent structures, the dimensions of the cubic unit cell were set to 20 Å. In the DFT calculations, all atoms and all the bonds are relaxed. The AlG structure includes 36 carbon atoms and 1 Al atom that was located at the center of the cluster structure. All dangling carbon atom bonds of the AlG were saturated with 15 Hydrogen (H) atoms to neutralize the charge on the structure. The kinetic energy cutoff for the description of Kohn–Sham orbitals and for the charge density and potential were set at 50 Ry and 400 Ry, respectively. The convergence threshold for each consecutive self-consistency step was set at $10^{-8}$ Ry and 7x7x1 Monkhorst-Pack grid were used for k-point sampling (44). The geometry of the structures was optimized and bond lengths were determined. Highest occupied molecular orbital (HOMO) and lowest unoccupied molecular orbital (LUMO) energies were calculated and the energy gap ($E_g$) was obtained by using the HOMO ($E_{HOMO}$) and LUMO ($E_{LUMO}$) energies.

$$E_g = E_{LUMO} - E_{HOMO} \quad (1)$$

The adsorption energies ($E_{ads}$) were calculated by the following equation.

$$E_{ads} = E_{system} - E_{adsorptive} - E_{adsorbed} \quad (2)$$

where $E_{system}$ refers to the energy of $C_2H_4$/AlG or 1-MCP/AlG, the adsorptive energy ($E_{adsorptive}$) is the energy of AlG and $E_{adsorbed}$ is the energy of ethylene or 1-MCP. Density of states (DOS) and electrostatic potential (ESP) were calculated. The global indices of reactivity of the structures were investigated by calculating the chemical hardness (η), chemical potential (μ) and electrophilicity (ω) (45-47).

$$\eta = \frac{(E_{LUMO} - E_{HOMO})}{2} \quad (3)$$

$$\mu = -\frac{(E_{LUMO} + E_{HOMO})}{2} \quad (4)$$

$$\omega = \frac{\mu^2}{2\eta} \quad (5)$$

## 3. RESULTS AND DISCUSSION

### 3.1. The structure of ethylene, 1-MCP and AlG

The structure of ethylene, 1-MCP molecules and AlG, which was optimized by DFT calculations, was presented in Fig. 1 and the optimized bond lengths were listed in Table 1, respectively. From Table 1, 1-MCP, being a cyclopropene, has a shorter π-bond of 1.2994 Å ($C1_M$-$C3_M$) than that of the ethylene, 1.3317 Å. A similar difference was also observed between the C-H bonds of 1-MCP (1.0828 Å) and ethylene (1.0907 Å).

The optimized structure of AlG was presented from the top and the side views in Fig. 1(c) and Fig. 1(d). The 2 $sp^2$ - 3 $sp^2$ hybridization of the three carbon atoms in the graphene with the aluminum atom disrupts the planarity at an angle of 120 degrees and turned the planar structure of graphene into an umbrella-like structure. Moreover, the empty $p_z$ hybrid orbital of octet-deficient aluminum gave the AlG extraordinary properties such as Lewis acidity (48). The calculated bond lengths of the Al atom with the neighboring C atoms (1,846 Å) were slightly greater than the C-C bond length in the pristine graphene structure (Table 1). At the same time, the C-C bond lengths of the other neighboring C atoms were different from those of the graphene. In other words, since the remarkable negative potential distributes on the location of the Al atom, in the aluminum-centered-doped graphene (AlG) the aromatic homogeneity of the pure graphene was changed, relatively.

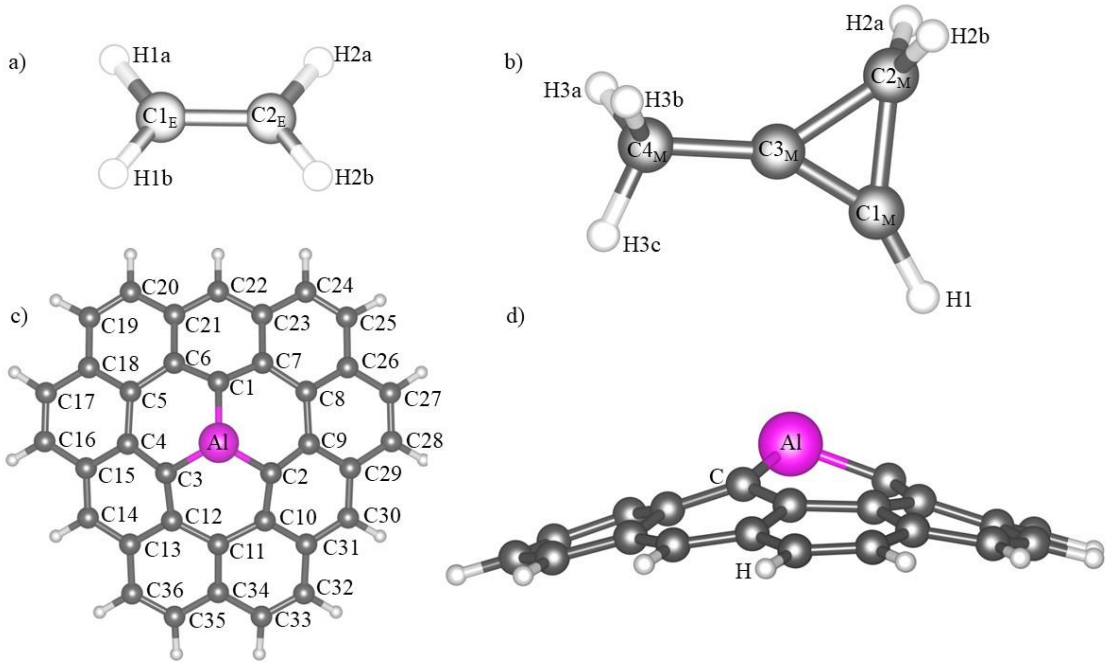


**Figure 1:** The optimized geometric structure of ethylene (a), 1-MCP (b) and top (c) and side (d) views of AlG.

**Table 1:** The optimized bond lengths of ethylene, 1-MCP and AlG.

| $C_2H_4$ (Å) | | 1-MCP (Å) | | AlG (Å) | | | |
|---|---|---|---|---|---|---|---|
| $C1_E$-$C2_E$ | 1.3317 | $C1_M$-$C2_M$ | 1.5109 | C1-Al | 1.8466 | C4-C5 | 1.4781 |
| $C1_E$-H1a | 1.0907 | $C2_M$-$C3_M$ | 1.5117 | C2-Al | 1.8466 | C5-C6 | 1.4780 |
| | | $C1_M$-$C3_M$ | 1.2994 | C3-Al | 1.8466 | C6-C21 | 1.4397 |
| | | $C3_M$-$C4_M$ | 1.4716 | C3-C4 | 1.4114 | C19-C20 | 1.3652 |

### 3.2. Orbital Analysis of Ethylene, 1-MCP and AlG

Frontier molecular orbitals (HOMO and LUMO) and the HOMO and LUMO energies and the DOS of ethylene, 1-MCP and AlG were calculated and presented in Fig. 2, Fig. 3, Fig. 4 and Table 2, respectively. As can be seen in Fig. 2, the HOMO of ethylene was symmetrically localized on the $C1_E$-$C2_E$ bond and the LUMO was on the opposite side. The HOMO of 1-MCP was relatively located more on the carbon atom $C1_M$ due to the inductive effect of the methyl group (Fig. 3). The energy gap ($E_g$) of 1-

MCP, that was calculated by using Eq. (1), ($E_g$ = 5.01 eV) was smaller than that of ethylene ($E_g$= 5.68 eV).

In Fig. 4, the HOMO of AlG was partially localized over the aromatic π-clouds in the carbon rings, while the LUMO was mainly centered over the Al atom of the AlG. Depending on that the greatest extension of LUMO shape was on the Al atom, the electrophilic reactions between ethylene or 1-MCP and AlG were expected to be observed on the Al atom. The HOMO and LUMO energies of AlG were -4.47 and -3.01 eV, respectively and the energy gap was 1.48 eV (Table 3). In addition to these, due to the relatively lower LUMO energy with respect to that of ethylene and 1-MCP, AlG can be considered to be a good electron acceptor to adsorb the ethylene or 1-MCP molecules.

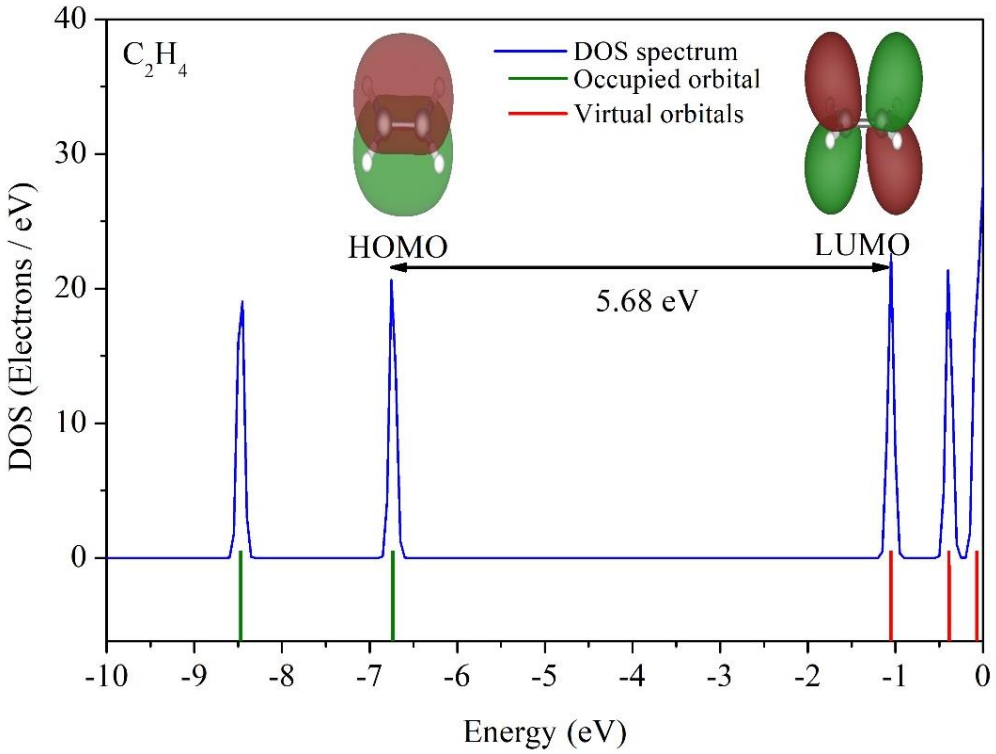


**Figure 2:** The graph of DOS as a function of energy and the HOMO and LUMO and energy gap of ethylene.

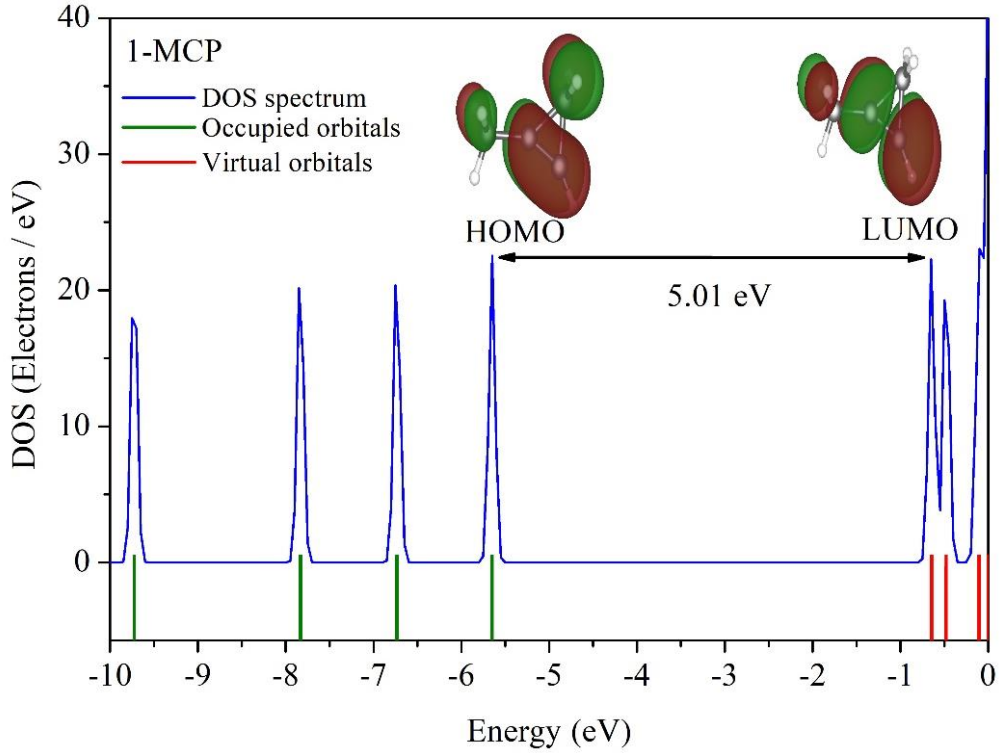


**Figure 3:** The graph of DOS as a function of energy and the HOMO and LUMO and energy gap of 1-MCP.

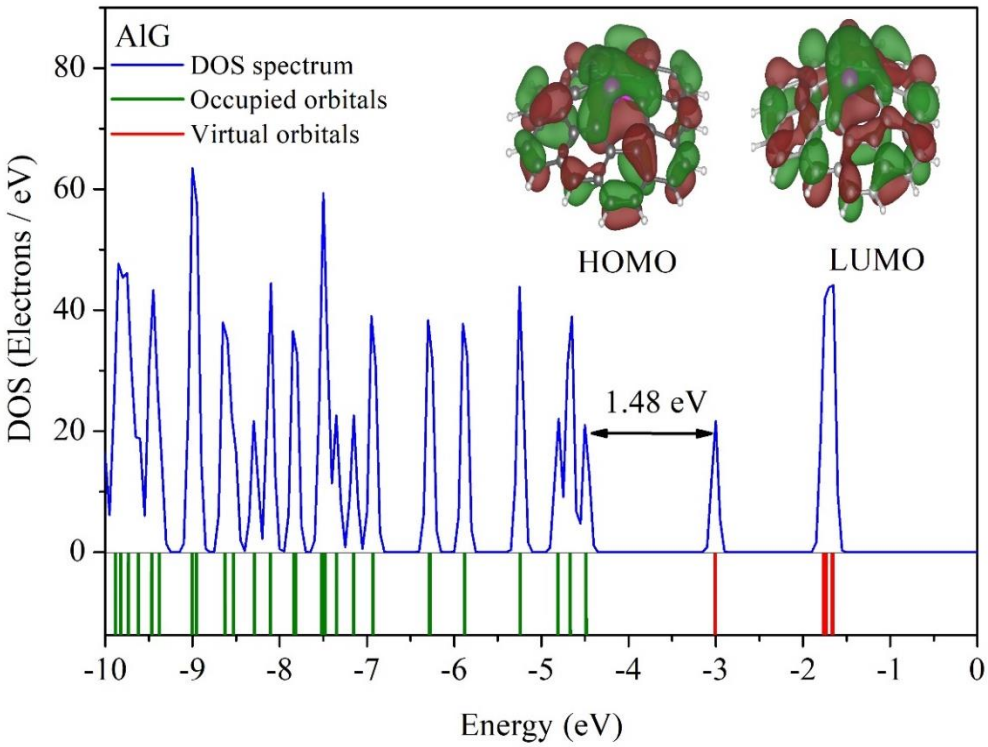


**Figure 4:** The graph of DOS as a function of energy and the HOMO and LUMO and energy gap of the AlG.

### 3.3. Adsorption of Ethylene and 1-MCP Molecules on AlG and Global Reactivity Analysis

Ethylene and 1-MCP can be physically and chemically adsorbed on AlG structure. In order to investigate both of these absorption mechanisms of ethylene and 1-MCP on AlG, the adsorption was analyzed by considering the two structurally optimized systems, that in the first one the adsorbed molecule was relatively nearer to AlG than that in the second one, for each of the adsorbed molecules. In this respect, to determine the corresponding chemical and physical adsorption distances between the adsorbed molecules and the adsorbent structure in the first step of the analysis, a series of structural geometry optimizations and energy convergence analyses were performed for each of the molecules. As a result, for the physical adsorption mechanism of ethylene and 1-MCP at position 1 (P1) (2.38 and 2.45 Å, respectively) and for the chemical adsorption mechanism of them at position 2 (P2) (2.12 and 2.09 Å, respectively) were determined and presented in Fig. 5-8.

Ethylene molecule is π-ligand and it bonded to AlG as $\eta^2$ bridging ligand. 1-MCP molecule was bonded to AlG by a coordinate covalent bond, due to both the inductive effect of the methyl group and the steric factor. These differences in the bonding were also confirmed by the difference in the bond lengths in the optimized structure (Table 2). According to Fig. 5, the ethylene molecule was physically adsorbed at a distance of 2.38 Å, while it was chemically absorbed as a $\eta^2$ bridging ligand at a bond length of 2.12 Å (Fig. 6). On the other hand, in Fig. 7, 1-MCP was physically adsorbed at a distance of 2.45 Å, while it was chemically adsorbed with a coordinated covalent bond with a bond length of 2.09 Å (Fig. 8). The difference in bond lengths highlights that 1-MCP was better adsorbed than ethylene on AlG.

The HOMO and LUMO energies of ethylene and 1-MCP on AlG ($C_2H_4$/AlG and 1-MCP/AlG, respectively) for P1 were -4.15, -2.61 eV and -4.18, -2.69 eV, and for P2 were -4.19, -2.63 eV and -4.09, -2.57 eV, respectively (Table 3). Since aluminum atom has one valence electron less than that of carbon atom, AlG is an electron-deficient system. During the adsorption, there occurs an electron transfer from ethylene and 1-MCP molecules onto AlG. It was observed that ethylene forms a π-complex (a trigonal ring), and on the other hand, the bonding structure of 1-MCP over $C1_M$ carbon was relatively more stable, due to the steric and inductive effects of the methyl group.

Comparing the DOS of AlG (Fig. 4) to that of the $C_2H_4$/AlG and 1-MCP/AlG (Fig. 5, 6, 7, 8), a change in the confirmation of hybridization was determined. The $E_g$ values of $C_2H_4$/AlG and 1-MCP/AlG structures were slightly greater than that of AlG for both positions (P1 and P2) (Table 3).

The global indices of reactivity of ethylene, 1-MCP, AlG, $C_2H_4$/AlG and 1-MCP/AlG were presented in Table 3, where chemical hardness (η), chemical potential (μ), electrophilicity (ω) were calculated using Eq. 3-5, respectively. The hardness of AlG decreases by the adsorption of ethylene or 1-MCP. The electrophilicity of AlG was higher than that of ethylene and 1-MCP. The adsorption energy ($E_{ads}$) of ethylene and 1-MCP, that was defined in Eq.2, was –60.16 kJ/mol and -7.32 kJ/mol for P1 and 19.34 kJ/mol and 56.53 kJ/mol for P2, respectively. The larger the adsorption energy and the shorter the distance between the adsorbed molecule and AlG suggest that 1-MCP has a better chemical bonding than ethylene.

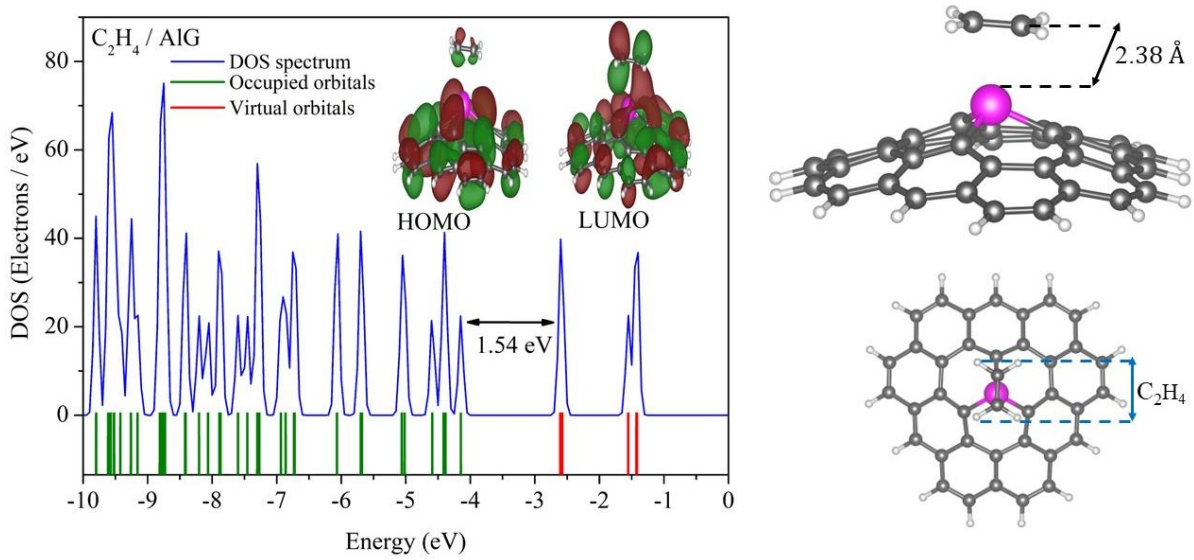


**Figure 5:** The graph of DOS as a function of energy and the HOMO and LUMO and energy gap of the $C_2H_4$/AlG for position 1.

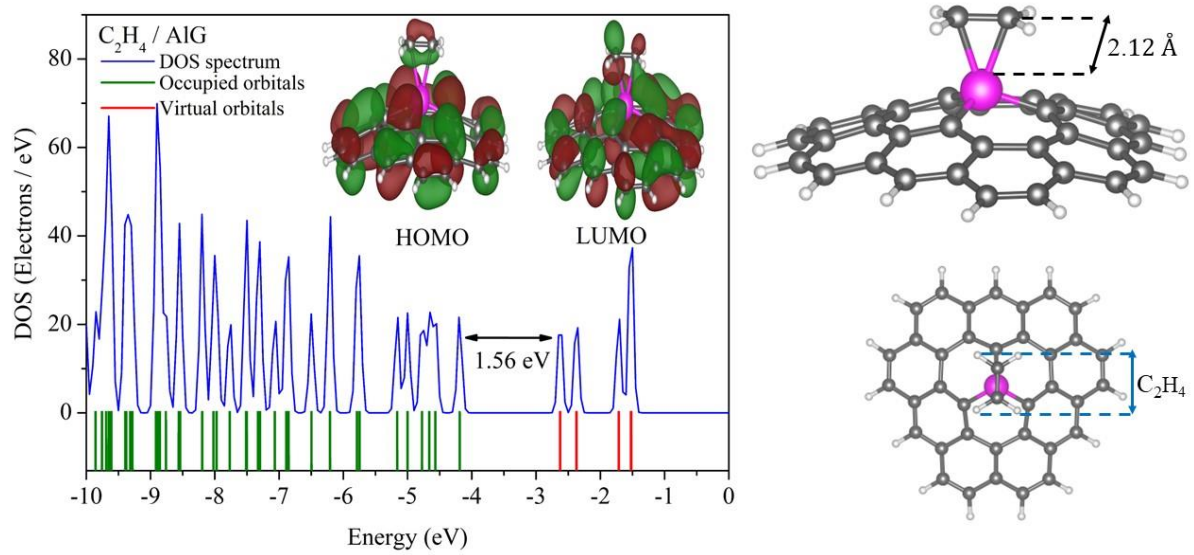


**Figure 6:** The graph of DOS as a function of energy and the HOMO and LUMO and energy gap of the $C_2H_4$/AlG for position 2.

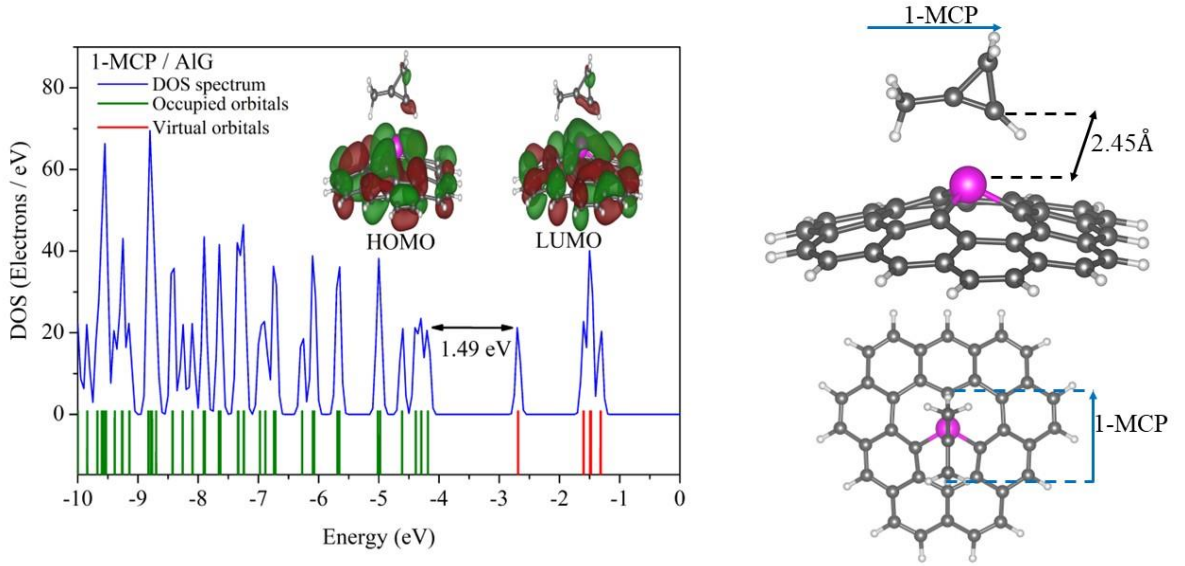


**Figure 7:** The graph of DOS as a function of energy and the HOMO and LUMO and energy gap of the 1-MCP/AlG for position 1.

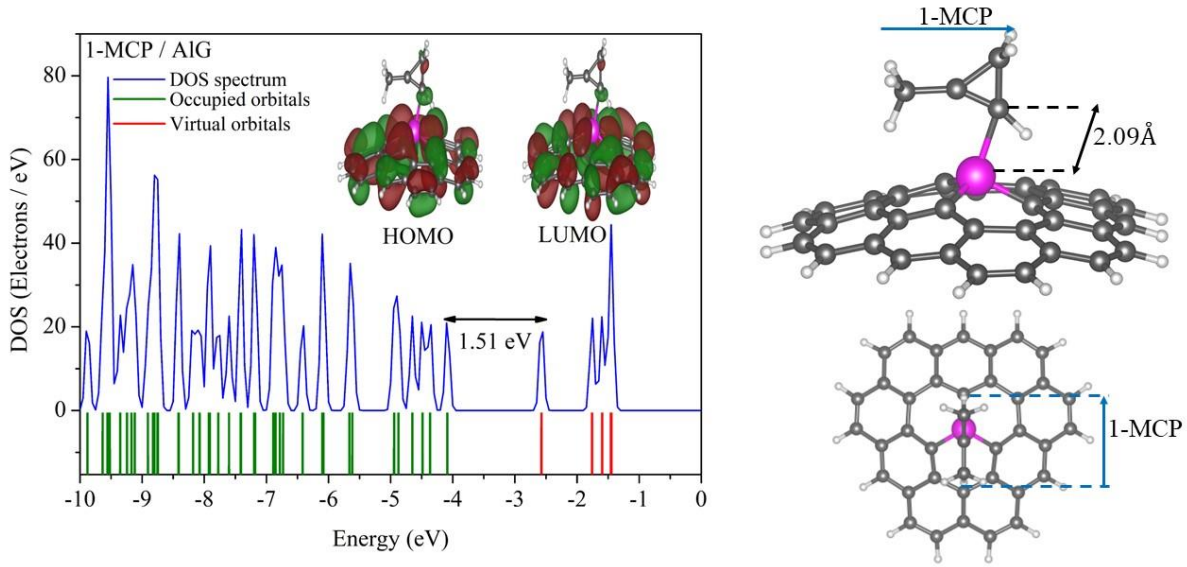


**Figure 8:** The graph of DOS as a function of energy and the HOMO and LUMO and energy gap of the 1-MCP/AlG for position 2.

**Table 2:** The optimized bond lengths of $C_2H_4$/AlG and 1-MCP/AlG for position 1 (P1) and position 2 (P2).

| | **$C_2H_4$ / AlG (P1) (Å)** | **$C_2H_4$ / AlG (P2) (Å)** | **1-MCP /AlG (P1) (Å)** | **1-MCP/ AlG (P2) (Å)** |
|---|---|---|---|---|
| C1-Al | 1.8873 | 1.8489 | 1.8537 | 1.8354 |
| C2-Al | 1.8745 | 1.8350 | 1.8550 | 1.8288 |
| C3-Al | 1.8752 | 1.8365 | 1.8556 | 1.8288 |
| C3-C4 | 1.4082 | 1.3998 | 1.4063 | 1.4055 |
| C4-C5 | 1.4762 | 1.4880 | 1.4758 | 1.4874 |
| C5-C6 | 1.4766 | 1.4873 | 1.4752 | 1.4838 |
| C6-C21 | 1.4416 | 1.4332 | 1.4380 | 1.4386 |
| C19-C20 | 1.3641 | 1.3605 | 1.3700 | 1.3645 |

**Table 3:** The adsorption energy ($E_{ads}$), HOMO and LUMO energies ($E_{HOMO}$, $E_{LUMO}$), energy gap ($E_g$), chemical hardness (η), chemical potential (μ) and electrophilicity (ω) of ethylene, 1-MCP, AlG, $C_2H_4$/AlG and 1-MCP/Alg position 1 (P1) and position 2 (P2).

| | **$C_2H_4$** | **1-MCP** | **AlG** | **$C_2H_4$/AlG (P1)** | **$C_2H_4$/AlG (P2)** | **1-MCP/AlG (P1)** | **1-MCP/AlG (P2)** |
|---|---|---|---|---|---|---|---|
| $E_{ads}$ (kJ $mol^{-1}$) | | | | -60.16 | 19.34 | -7.32 | 56.53 |
| $E_{HOMO}$ (eV) | -6.73 | -5.65 | -4.47 | -4.15 | -4.19 | -4.18 | -4.09 |
| $E_{LUMO}$ (eV) | -1.05 | -0.64 | -3.01 | -2.61 | -2.63 | -2.69 | -2.57 |
| $E_q$ (eV) | 5.68 | 5.01 | 1.48 | 1.54 | 1.56 | 1.49 | 1.51 |
| η (eV) | 2.84 | 2.50 | 0.74 | 0.77 | 0.78 | 0.75 | 0.76 |
| μ (eV) | 3.89 | 3.15 | 3.75 | 3.38 | 3.41 | 3.43 | 3.33 |
| ω (eV) | 2.67 | 1.98 | 9.51 | 7.40 | 7.42 | 7.89 | 7.31 |

### 3.4. The ESP Analysis

The ESP map conveys information about possible reaction sites of electrophilic or nucleophilic attacks. The three-dimensional ESP of ethylene and 1-MCP on AlG were calculated and the ESP maps were presented in Fig. 9 by a blue-green-yellow colored spectrum of the cross-sectional plane, that is passing through the carbon atoms of ethylene or 1-MCP and the Al atom of AlG. The yellow color, that indicates a negative ESP, is the lower potential region that the charge is depleted most and the blue color, that indicates a positive ESP, is the higher potential. Additionally, the graded black curves on the cross-sectional view of the ESP (Fig. 9) represent the equal ESP curves. Accordingly, the ESP maps shows that the Al atom is on a level of lower potential, which indicates a higher nucleophilic reactive site. In Fig. 9, the ESP changes color around the C, H and Al atoms.

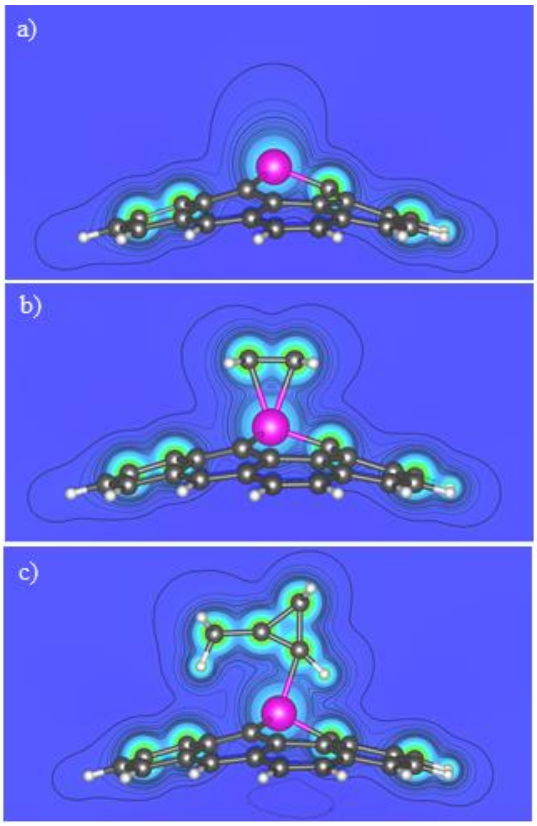


**Figure 9:** The electrostatic potential (ESP) map of (a) AlG, (b) $C_2H_4$/AlG and (c) 1-MCP/AlG. The graded black curves represent the equal ESP curves.

## 4. CONCLUSION

In the present study, the adsorption and activity of ethylene and 1-MCP molecules on Al-doped graphene (AlG) as a theoretical point of view were characterized through structural geometry optimization, HOMO and LUMO, adsorption energy, global reactivity and ESP calculations by using the DFT calculations.

The HOMO was located on the alkene carbon atoms of the ethylene and 1-MCP molecules while LUMO was located on the aluminum atom in AlG. From the HOMO/LUMO graphs corresponding to the interactions of the studied molecules, it is seen that the carbons of the interacting ethylene contribute largely to the HOMO, while in 1-MCP, the interaction center is different due to the steric and inductive effects of the methyl group. Global reactivity analyses confirmed that Al-doped graphene treats as electron acceptor and so ethylene and 1-MCP molecules treat as electron donor. So, the chemical hardness of the Al-doped graphene (0.74 eV) is lower than that of ethylene and 1-MCP (2,84 and 2.50 eV, respectively) and also the values of electrophilicity index (9.91 eV) is higher than of the ethylene and 1-MCP (2.67 and 1.98 eV, respectively) molecules. The adsorption energies of the ethylene and 1-MCP molecules in interaction with Al-doped graphene were calculated as -60.16, 19.34, -7.32 and 56.53 eV for P1 and P2 adsorption mechanism, respectively. The chemical and physical adsorptions of these gas molecules by AlG were effectively confirmed by different analyses such as ESP and DOS. According to these results, AlG is capable to be a new gas sensor for the adsorption of both ethylene and 1-MCP molecules. Moreover, these analyses implied that AlG is a better adsorbent/gas sensor for 1-MCP molecule than ethylene molecule.

## 5. CONFLICT OF INTEREST

The authors declare no competing interests.

## 6. ACKNOWLEDGMENTS

The numerical calculations reported in this paper were fully performed at TUBITAK ULAKBIM, High Performance and Grid Computing Center (TRUBA resources).

## 7. REFERENCES

1. Yang SF, Hoffman NE. Ethylene biosynthesis and its regulation in higher plants. Annu Rev Plant Physiol [Internet]. 1984 Jun;35(1):155–89. Available from: <URL>.

2. Zimmermann H, Walzl R. Ethylene. In: Ullmann's Encyclopedia of Industrial Chemistry [Internet]. Weinheim, Germany: Wiley-VCH Verlag GmbH & Co. KGaA; 2000. Available from: <URL>.

3. Dias C, Ribeiro T, Rodrigues AC, Ferrante A, Vasconcelos MW, Pintado M. Improving the ripening process after 1-MCP application: Implications and strategies. Trends Food Sci Technol [Internet]. 2021 Jul;113:382–96. Available from: <URL>.

4. Magid RM, Clarke TC, Duncan CD. Efficient and convenient synthesis of 1-methylcyclopropene. J

Org Chem [Internet]. 1971 May 1;36(9):1320–1. Available from: <URL>.

5. Blankenship SM, Dole JM. 1-Methylcyclopropene: A review. Postharvest Biol Technol [Internet]. 2003 Apr 1;28(1):1–25. Available from: <URL>.

6. Sisler EC, Serek M. Inhibitors of ethylene responses in plants at the receptor level: Recent developments. Physiol Plant [Internet]. 1997 Jul 28;100(3):577–82. Available from: <URL>.

7. Watkins CB. The use of 1-methylcyclopropene (1-MCP) on fruits and vegetables. Biotechnol Adv [Internet]. 2006 Jul;24(4):389–409. Available from: <URL>.

8. Ekinci N, Şeker M, Aydın F, Gündoğdu MA. Possible chemical mechanism and determination of inhibitory effects of 1-MCP on superficial scald of the Granny Smith apple variety. Turkish J Agric For [Internet]. 2016;40:38–44. Available from: <URL>.

9. Liu R, Lai T, Xu Y, Tian S. Changes in physiology and quality of Laiyang pear in long time storage. Sci Hortic [Internet]. 2013 Feb;150:31–6. Available from: <URL>.

10. Serek M, Sisler EC, Reid MS. Effects of 1-MCP on the vase life and ethylene response of cut flowers. Plant Growth Regul [Internet]. 1995 Jan;16(1):93–7. Available from: <URL>.

11. Dong M, Wen G, Li J, Wang T, Huang J, Li Y, et al. Determination of 1-methylcyclopropene residues in vegetables and fruits based on iodine derivatives. Food Chem [Internet]. 2021 Oct;358:129854. Available from: <URL>.

12. Lee YS, Beaudry R, Kim JN, Harte BR. Development of a 1-Methylcyclopropene (1-MCP) sachet release system. J Food Sci [Internet]. 2006 Jan 31;71(1). Available from: <URL>.

13. Novoselov KS, Geim AK, Morozov S V., Jiang D, Zhang Y, Dubonos S V., et al. Electric field effect in atomically thin carbon films. Science (80- ) [Internet]. 2004 Oct 22;306(5696):666–9. Available from: <URL>.

14. Geim AK, Novoselov KS. The rise of graphene. Nat Mater [Internet]. 2007 Mar;6(3):183–91. Available from: <URL>.

15. Rad AS. First principles study of Al-doped graphene as nanostructure adsorbent for $NO_2$ and $N_2O$: DFT calculations. Appl Surf Sci [Internet]. 2015 Dec;357:1217–24. Available from: <URL>.

16. Sun Y, Chen L, Zhang F, Li D, Pan H, Ye J. First-principles studies of HF molecule adsorption on intrinsic graphene and Al-doped graphene. Solid State Commun [Internet]. 2010 Oct;150(39–40):1906–10. Available from: <URL>.

17. Rouhani M. DFT study on adsorbing and detecting possibility of cyanogen chloride by pristine, B, Al, Ga, Si and Ge doped graphene. J Mol Struct [Internet]. 2019 Apr;1181:518–35. Available from: <URL>.

18. Rad AS, Shadravan A, Soleymani AA, Motaghedi N. Lewis acid-base surface interaction of some boron compounds with N-doped graphene; first principles study. Curr Appl Phys [Internet]. 2015 Oct;15(10):1271–7. Available from: <URL>.

19. Zhou X, Zhao C, Wu G, Chen J, Li Y. DFT study on the electronic structure and optical properties of N, Al, and N-Al doped graphene. Appl Surf Sci [Internet]. 2018 Nov;459:354–62. Available from: <URL>.

20. Esrafili MD, Saeidi N, Nematollahi P. A DFT study on $SO_3$ capture and activation over Si- or Al-doped graphene. Chem Phys Lett [Internet]. 2016 Aug;658:146–51. Available from: <URL>.

21. Singh D, Kumar A, Kumar D. Adsorption of small gas molecules on pure and Al-doped graphene sheet: A quantum mechanical study. Bull Mater Sci [Internet]. 2017 Oct 3;40(6):1263–71. Available from: <URL>.

22. Gecim G, Ozekmekci M, Fellah MF. Ga and Ge-doped graphene structures: A DFT study of sensor applications for methanol. Comput Theor Chem [Internet]. 2020 Jun;1180:112828. Available from: <URL>.

23. Tian YH, Hu S, Sheng X, Duan Y, Jakowski J, Sumpter BG, et al. Non-transition-metal catalytic system for $N_2$ reduction to $NH_3$: A density functional theory study of Al-doped graphene. J Phys Chem Lett [Internet]. 2018 Feb 1;9(3):570–6. Available from: <URL>.

24. Jappor HR, Khudair SAM. Al-doped graphene as a sensor for harmful gases (CO, $CO_2$, $NH_3$, NO, $NO_2$ and $SO_2$). Sens Lett [Internet]. 2017 Dec 1;15(12):1023–30. Available from: <URL>.

25. Rad AS, Pouralijan Foukolaei V. Density functional study of Al-doped graphene nanostructure towards adsorption of CO, $CO_2$ and $H_2O$. Synth Met [Internet]. 2015 Dec;210:171–8. Available from: <URL>.

26. Ao ZM, Yang J, Li S, Jiang Q. Enhancement of CO detection in Al doped graphene. Chem Phys Lett [Internet]. 2008 Aug;461(4–6):276–9. Available from: <URL>.

27. Rad AS. Al-doped graphene as a new nanostructure adsorbent for some halomethane compounds: DFT calculations. Surf Sci [Internet]. 2016 Mar;645:6–12. Available from: <URL>.

28. Zhao W, Meng QY. Adsorption of methane on pristine and Al-doped graphene: A comparative study via first-principles calculation. Adv Mater Res [Internet]. 2012 Dec;602–604:870–3. Available from: <URL>.

29. Rastegar SF, Peyghan AA, Hadipour NL. Response of Si- and Al-doped graphenes toward HCN: A computational study. Appl Surf Sci [Internet]. 2013 Jan;265:412–7. Available from:

<URL>.

30. Chi M, Zhao YP. Adsorption of formaldehyde molecule on the intrinsic and Al-doped graphene: A first principle study. Comput Mater Sci [Internet]. 2009 Oct;46(4):1085–90. Available from: <URL>.

31. Zhang T, Sun H, Wang F, Zhang W, Ma J, Tang S, et al. Electric-field controlled capture or release of phosgene molecule on graphene-based materials: First principles calculations. Appl Surf Sci [Internet]. 2018 Jan;427:1019–26. Available from: <URL>.

32. Rastegar SF, Hadipour NL, Tabar MB, Soleymanabadi H. DFT studies of acrolein molecule adsorption on pristine and Al- doped graphenes. J Mol Model [Internet]. 2013 Sep 22;19(9):3733–40. Available from: <URL>.

33. Rad AS, Jouibary YM, Foukolaei VP, Binaeian E. Study on the structure and electronic property of adsorbed guanine on aluminum doped graphene: First principles calculations. Curr Appl Phys [Internet]. 2016 May;16(5):527–33. Available from: <URL>.

34. Rad AS, Alijantabar Aghouzi S, Motaghedi N, Maleki S, Peyravi M. Theoretical study of chemisorption of cyanuric fluoride and S-triazine on the surface of Al-doped graphene. Mol Simul [Internet]. 2016 Dec 11;42(18):1519–27. Available from: <URL>.

35. Hohenberg P, Kohn W. Inhomogeneous electron gas. Phys Rev [Internet]. 1964 Nov 9;136(3B):B864–71. Available from: <URL>.

36. Kohn W, Sham LJ. Self-consistent equationsincluding exchange and correlation effects. Phys Rev [Internet]. 1965 Nov 15;140(4A):A1133–8. Available from: <URL>.

37. Giannozzi P, Baroni S, Bonini N, Calandra M, Car R, Cavazzoni C, et al. Quantum espresso: A modular and open-source software project for quantum simulations of materials. J Phys Condens Matter [Internet]. 2009 Sep 30;21(39):395502. Available from: <URL>.

38. Giannozzi P, Andreussi O, Brumme T, Bunau O, Buongiorno Nardelli M, Calandra M, et al. Advanced capabilities for materials modelling with quantum espresso. J Phys Condens Matter [Internet]. 2017 Nov 22;29(46):465901. Available from: <URL>.

39. Giannozzi P, Baseggio O, Bonfà P, Brunato D, Car R, Carnimeo I, et al. Quantum espresso toward the exascale. J Chem Phys [Internet]. 2020 Apr 21;152(15). Available from: <URL>.

40. Vanderbilt D. Soft self-consistent pseudopotentials in a generalized eigenvalue formalism. Phys Rev B [Internet]. 1990 Apr 15;41(11):7892–5. Available from: <URL>.

41. Perdew JP, Burke K, Ernzerhof M. Generalized Gradient Approximation Made Simple. Phys Rev Lett [Internet]. 1996 Oct 28;77(18):3865–8. Available from: <URL>.

42. Kokalj A. Computer graphics and graphical user interfaces as tools in simulations of matter at the atomic scale. Comput Mater Sci [Internet]. 2003 Oct;28(2):155–68. Available from: <URL>.

43. Momma K, Izumi F. *VESTA 3* for three-dimensional visualization of crystal, volumetric and morphology data. J Appl Crystallogr [Internet]. 2011 Dec 1;44(6):1272–6. Available from: <URL>.

44. Monkhorst HJ, Pack JD. Special points for Brillouin-zone integrations. Phys Rev B [Internet]. 1976 Jun 15;13(12):5188–92. Available from: <URL>.

45. Makov G. Chemical hardness in density functional theory. J Phys Chem [Internet]. 1995 Jun 1;99(23):9337–9. Available from: <URL>.

46. Pearson RG. The electronic chemical potential and chemical hardness. J Mol Struct THEOCHEM [Internet]. 1992 Mar;255:261–70. Available from: <URL>.

47. Chattaraj PK, Parr RG. Density functional theory of chemical hardness. In: Chemical Hardness [Internet]. Berlin/Heidelberg: Springer-Verlag; p. 11–25. Available from: <URL>.

48. Coster D, Blumenfeld AL, Fripiat JJ. Lewis acid sites and surface aluminum in aluminas and zeolites: A high-resolution NMR study. J Phys Chem [Internet]. 1994 Jun 1;98(24):6201–11. Available from: <URL>.